The following Communications have been judged by at least two referees to be "very important papers" and will be published online at www.angewandte.org soon:

*H. Jiang, P. Elsner, K. L. Jensen, A. Falcicchio, V. Marcos, K. A. Jørgensen**
Achieving Molecular Complexity by Organocatalytic One-Pot Strategies: A Fast Entry for the De Novo Synthesis of Sphingoids, Amino Sugars, and Polyhydroxylated α-Amino Acids

*T. J. Kucharski, Z. Huang, Q.-Z. Yang, Y. Tian, N. C. Rubin, C. D. Concepcion, R. Boulatov**
Kinetics of Thiol/Disulfide Exchange Correlates Weakly with the Restoring Force in the Disulfide Moiety

*W. Xu, X. Xue, T. Li, H. Zeng, X. Liu**
Ultrasensitive and Selective Colorimetric DNA Detection by Nicking Endonuclease-Assisted Nanoparticle Amplification

H. Ueda, H. Satoh, K. Matsumoto, K. Sugimoto, T. Fukuyama, H. Tokuyama**
Total Synthesis of (+)-Haplophytine

G. A. Zelada, J. Riu, A. Düzgün, F. X. Rius**
Immediate Detection of Living Bacteria at Ultra-Low Concentrations Using a Carbon-Nanotube-Based Potentiometric Aptasensor

*K. Fuchibe, T. Kaneko, K. Mori, T. Akiyama**
Expedient Synthesis of N-Fused Indoles: A C–F Activation and C–H Insertion Approach

A. Giannis, P. Heretsch, V. Sarli, A. Stößel*
Synthesis of Cyclopamine Using a Biomimetic and Diastereoselective Approach

W. A. Chalifoux, R. McDonald, M. J. Ferguson, R. R. Tykwinski
***tert*-Butyl Endcapped Polyynes: Crystallographic Evidence of Reduced Bond-Length Alternation**

Author Profile

"A good work day begins with a new and exciting experimental result.
The biggest challenge facing chemists is to understand the results and to convince other chemists that the unexpected chemical product was in fact desired. …"
This and more about Hans-Achim Wagenknecht can be found on page 5788.

Books

Highlights

Alkaline Earth Metal Catalysis

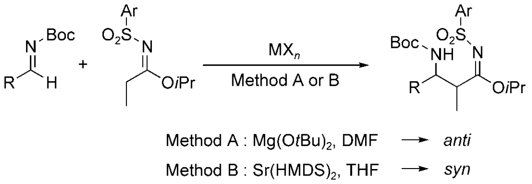

Trend-setting: Alkaline earth metals are good catalysts for a number of direct addition reactions with carbonyl compounds. In Mannich reactions the stereochemical outcome can be controlled by the reaction conditions and the alkaline earth metal used (see scheme: Boc = *tert*-butoxycarbonyl, HMDS = hexamethyldisilazide).

Electronic Structure

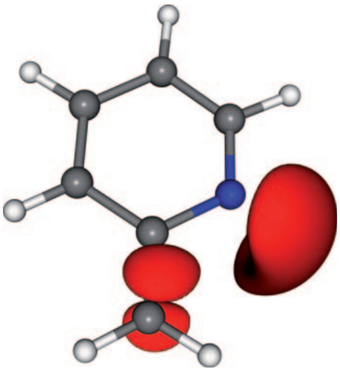

In perfect resonance: The electron density distribution is typically used to analyze chemical bonding, even if strong electron delocalization occurs. The electron densities and electric potentials of picoline and the picolyl anion (see picture) have been analyzed and a detailed description of picolyl lithium complexes has been derived. The next goal is to predict chemical reactivity from electron density.

Reviews

Cancer Research

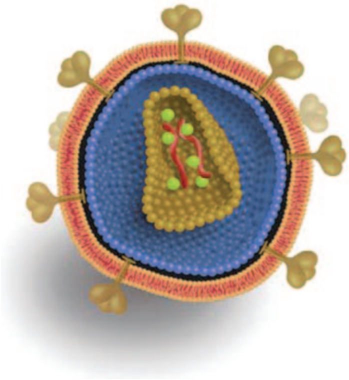

Viruses are the uniting theme of the 2008 Nobel Prize for Physiology or Medicine. Françoise Barré-Sinoussi and Luc Montagnier received their Prize for the discovery of the human immunodeficiency virus (HIV), and Harald zur Hausen identified that cervical cancer is triggered by papillomaviruses. The Nobel Laureates describe their research first-hand.

HIV/AIDS

For the USA and Canada:
ANGEWANDTE CHEMIE International Edition (ISSN 1433-7851) is published weekly by Wiley-VCH, PO Box 191161, 69451 Weinheim, Germany. Air freight and mailing in the USA by Publications Expediting Inc., 200 Meacham Ave., Elmont, NY 11003. Periodicals postage paid at Jamaica, NY 11431. US POSTMASTER: send address changes to *Angewandte Chemie*, Wiley-VCH, 111 River Street, Hoboken, NJ 07030. Annual subscription price for institutions: US$ 7225/6568 (valid for print and electronic / print or electronic delivery); for individuals who are personal members of a national chemical society prices are available on request. Postage and handling charges included. All prices are subject to local VAT/sales tax.

Communications

Hydrogen Storage

J. Wang, T. Liu, G. Wu, W. Li, Y. Liu, C. M. Araújo, R. H. Scheicher, A. Blomqvist, R. Ahuja, Z. Xiong, P. Yang, M. Gao, H. Pan, P. Chen* — **5828 – 5832**

Potassium-Modified $Mg(NH_2)_2/2\,LiH$ System for Hydrogen Storage

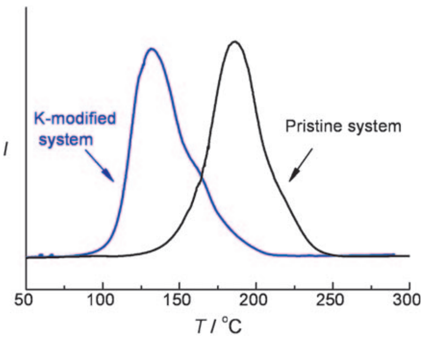

Using KH as an additive to $Mg(NH_2)_2/LiH$ drastically improves hydrogen desorption, which begins at ca. 80 °C (see graph). Circa 5 wt % of hydrogen can be reversibly desorbed and absorbed at about 107 °C. The presence of potassium in the reacting system weakens the amide N–H and imide Li–N bonds, leading to enhanced reaction kinetics.

Protein Patterns

N. Ballav, H. Thomas, T. Winkler, A. Terfort, M. Zharnikov* — **5833 – 5836**

Making Protein Patterns by Writing in a Protein-Repelling Matrix

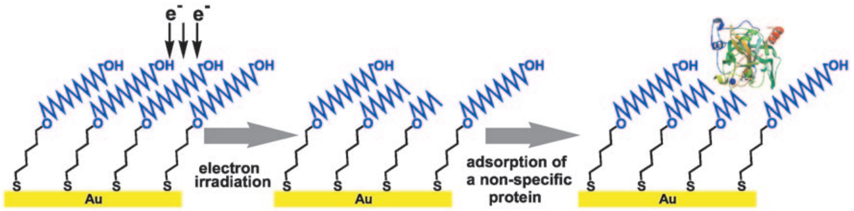

Write on target: An efficient and versatile approach to fabricate protein patterns of any shape on a variable length scale is developed. The patterns are directly written in an oligo- or poly(ethylene glycol)-based protein-repelling film by electron-beam lithography.

Boride Ligands

H. Braunschweig,* R. D. Dewhurst, K. Kraft, K. Radacki — **5837 – 5840**

Low-Coordinate Boride Ligands: A True Trimetalloborane

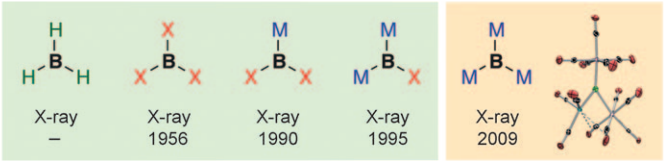

Boron trifecta: The first true trimetalloborane has been synthesized by simple salt elimination from a dimanganese bromoborylene and $Na[Co(CO)_4]$. The complex was structurally characterized, and features only first-row transition metals, a planar boron atom, and two semi-bridging CO ligands between the cobalt and one manganese atom (see picture).

Solid-Phase Synthesis

M. Mentel, A. M. Schmidt, M. Gorray, P. Eilbracht, R. Breinbauer* — **5841 – 5844**

Polystyrene Sulfonyl Chloride: A Highly Orthogonal Linker Resin for the Synthesis of Nitrogen-Containing Heterocycles

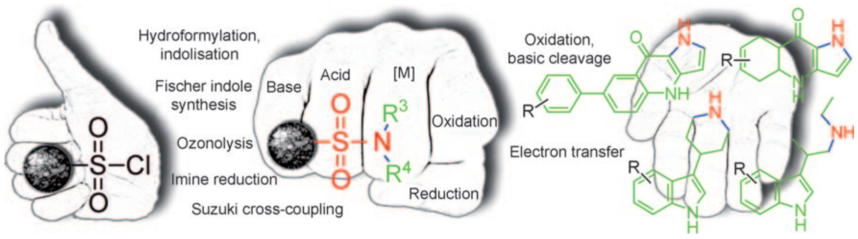

One linker, broad application: A simple sulfonamide linker for primary and secondary amines was used for the construction of small libraries of privileged indole and quinolone structures on a solid phase. After the synthesis, the products can be liberated ion a traceless manner under electron transfer conditions or according to a “safety catch” principle.

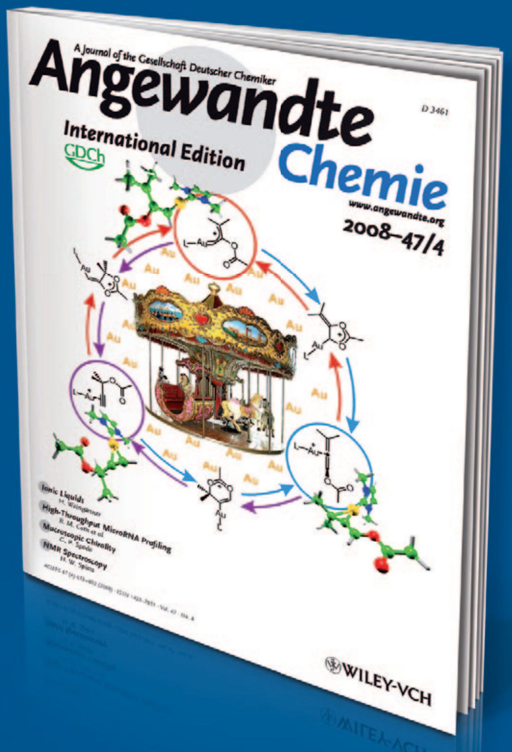
A Journal of the Gesellschaft Deutscher Chemiker
Angewandte Chemie
International Edition
GDCh
D 3461
www.angewandte.org
2008–47/4
Ionic Liquids
High-Throughput MicroRNA Profiling
Macroscopic Chirality
NMR Spectroscopy
WILEY-VCH

Bond-Stretch Isomerism

H. Shorafa, D. Mollenhauer, B. Paulus,
K. Seppelt* ______ 5845 – 5847

The Two Structures of the Hexafluorobenzene Radical Cation $C_6F_6^{\bullet +}$

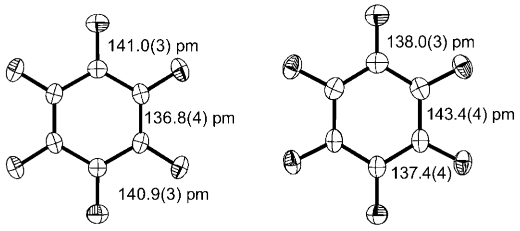

Quinoid Cation

Bisallyl Cation

Ring, ring! $C_6F_6^{\bullet +}$ $Os_2F_{11}^-$ and $C_6F_6^{\bullet +}Sb_2F_{11}^-$ have isomorphous crystal structures and each contain two different $C_6F_6^{\bullet +}$ cations. One is a quinoid structure, the other bisallyl structure. Calculations show that indeed two such Jahn–Teller distorted structures coexist with essentially the same energy. This seems to be a case of bond-stretch isomerism.

Synthetic Methods

A. S. K. Hashmi,* M. Rudolph, J. Huck,
W. Frey, J. W. Bats,
M. Hamzić ______ 5848 – 5852

Gold Catalysis: Switching the Pathway of the Furan-Yne Cyclization

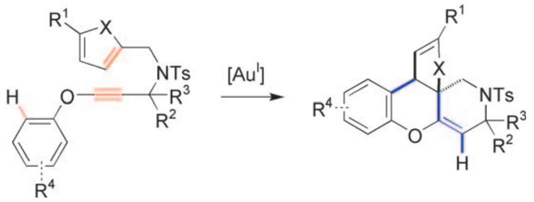

Changing tracks: By the use of alkynyl ethers as directing elements, the furan-yne cyclization enters a new reaction pathway. Instead of phenols, tetracycles containing two heteroatoms and two new stereocenters are formed (see scheme).

Protein–Protein Complex Inhibition

S. Sreeramulu, S. L. Gande, M. Göbel,
H. Schwalbe* ______ 5853 – 5855

Molecular Mechanism of Inhibition of the Human Protein Complex Hsp90–Cdc37, a Kinome Chaperone–Cochaperone, by Triterpene Celastrol

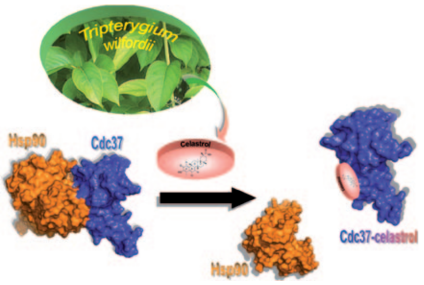

The correct target: The cell division cycle protein 37 (Cdc37) and the heat shock protein (Hsp90) are molecular chaperones crucial for the folding and stabilization of protein kinases including the oncogenic kinases. NMR studies show that celastrol, a recently identified triterpene targeting Hsp90, in fact binds to Cdc37 and disrupts the Cdc37–Hsp90 complex. Celastrol inactivates Cdc37 through a thiol-mediated mechanism.

Multicomponent Reactions

N. Elders, D. van der Born,
L. J. D. Hendrickx, B. J. J. Timmer,
A. Krause, E. Janssen, F. J. J. de Kanter,
E. Ruijter, R. V. A. Orru* ___ 5856 – 5859

The Efficient One-Pot Reaction of up to Eight Components by the Union of Multicomponent Reactions

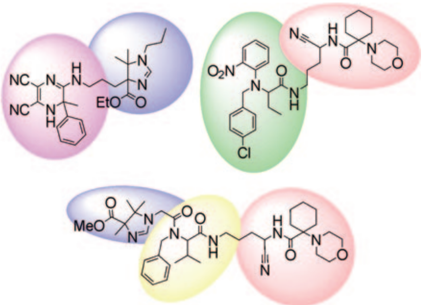

E = MCR²! The introduction of orthogonal functional groups in multicomponent reactions (MCRs) with unique solvent and functional-group compatibility enables their combination with other multicomponent reactions in one pot. The resulting novel 5- and 6CRs and an unprecedented 8CR afford very complex products in up to 80% yields (see picture), with up to nine new bond formations and eleven diversity points in a single reaction.

Contents

Natural Products

K. C. Nicolaou,* A. L. Nold,
H. Li ———————— **5860 – 5863**

Synthesis of the Monomeric Unit of the Lomaiviticin Aglycon

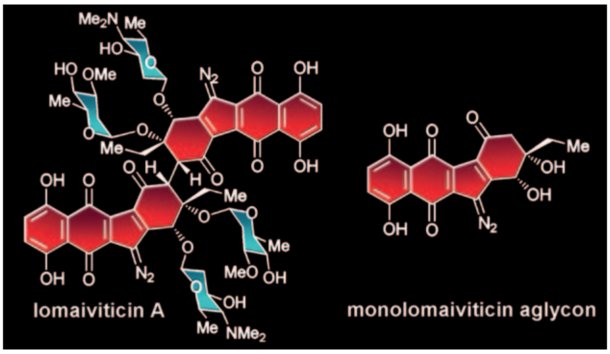

The right building blocks: The monomeric unit of the lomaiviticin aglycon (see structures) was synthesized through an enantioselective route featuring an Ullmann coupling, a benzoin-type cyclization, and a novel SmI_2-mediated allylic alcohol formal transposition.

Graphene

W. Zhang, J. Cui, C. Tao, Y. Wu, Z. Li, L. Ma,
Y. Wen, G. Li* ———————— **5864 – 5868**

A Strategy for Producing Pure Single-Layer Graphene Sheets Based on a Confined Self-Assembly Approach

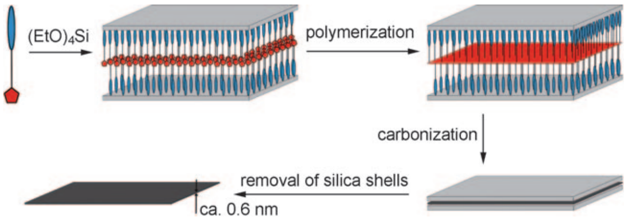

Carbon sandwich: When a pyrrole-containing surfactant is polymerized between layers of silica (see picture; pyrrole is red), subsequent carbonization and removal of the silica template yields large, pure, single-layer graphene sheets. The procedure, which employs mild conditions, is controllable and can be used to produce micrometer-sized graphene sheets on a gram scale.

Spontaneous Resolution

A. Lennartson,
M. Håkansson* ———————— **5869 – 5871**

Total Spontaneous Resolution of Five-Coordinate Complexes

Talking about a resolution: Bulk quantities of five-coordinate complexes have been resolved for the first time using zinc and cadmium diethyldithiocarbamate species. The stereochemical outcome can be controlled by seeding with the desired isomer, giving access to either enantiomer in high enantiomeric excess and yield.

Microelectrode Arrays

B. Bi, K. Maurer,
K. D. Moeller* ———————— **5872 – 5874**

Building Addressable Libraries: Site-Selective Lewis Acid (Scandium(III)) Catalyzed Reactions

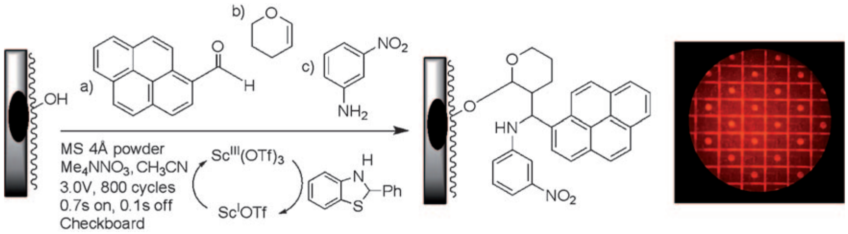

Reagent confinement: Lewis acid catalyzed reactions have been conducted on arrays with either 1024 or 12 544 microelectrodes cm^{-2}. A Sc^{III} species generated at the electrodes is employed as the Lewis acid, and the reagent is confined to the electrodes through the use of a solution-phase reductant. A multicomponent synthesis of a tetrahydropyran (see scheme), a Diels–Alder reaction, and an esterification reaction are all compatible with this strategy.

Magnetic Colloids

J. Liu, Z. K. Sun, Y. H. Deng,* Y. Zou, C. Y. Li, X. H. Guo, L. Q. Xiong, Y. Gao, F. Y. Li, D. Y. Zhao* ——— **5875–5879**

Highly Water-Dispersible Biocompatible Magnetite Particles with Low Cytotoxicity Stabilized by Citrate Groups

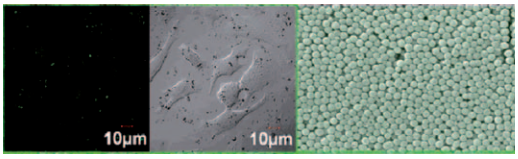

Uniform magnetite particles stabilized by citrate groups were successfully synthesized by a modified high-temperature solvothermal reaction. Cell imaging reveals that the water-dispersible particles can readily penetrate into cells without destroying them, indicating an excellent biocompatibility. A high enrichment capacity of the magnetite particles for separation of trace peptides is observed.

Synthetic Methods

W. Zhu, M. Mena, E. Jnoff, N. Sun, P. Pasau, L. Ghosez* ——— **5880–5883**

Multicomponent Reactions for the Synthesis of Complex Piperidine Scaffolds

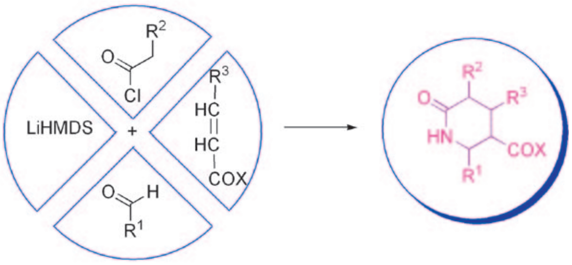

Creating diversity: Multicomponent reactions for the synthesis of complex piperidine scaffolds lead to high levels of skeletal, functional, and stereochemical diversity in an efficient way (see scheme, $X = OR$, NR_2). Connecting the acid chloride component to the dienophile generates polycyclic piperidine scaffolds by an intramolecular Diels–Alder reaction of the in situ generated azadienes.

Molecular Gates

A. Bernardos, E. Aznar, M. D. Marcos, R. Martínez-Máñez,* F. Sancenón, J. Soto, J. M. Barat,* P. Amorós* ——— **5884–5887**

Enzyme-Responsive Controlled Release Using Mesoporous Silica Supports Capped with Lactose

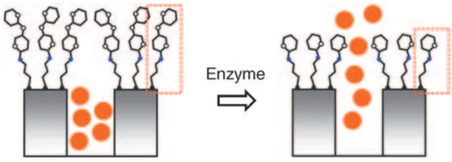

The great escape: A biocontrolled gated material has been prepared by grafting a lactose derivative onto the pore outlets of a mesoporous support. The galactosidase-induced hydrolysis of the β1→4 glycosidic bond in the lactose moiety (red box in picture) allows the release of a dye entrapped in the pores of the hybrid material to the bulk solution.

Magnetic Materials

L. Li,* Y. Feng, Y. Li, W. Zhao, J. Shi* ——— **5888–5892**

Fe_3O_4 Core/Layered Double Hydroxide Shell Nanocomposite: Versatile Magnetic Matrix for Anionic Functional Materials

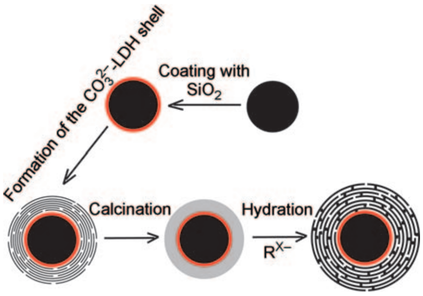

Layering up: The title nanocomposite shows high anion loading capacity. The demonstration of the assembly of a $W_7O_{24}^{6-}$ catalyst by this method may provide a general route to the facile and direct fabrication of composite structures with magnetic cores and shells functionalized with various anions (see scheme; LDH = layered double hydroxide).

Spirocyclization

T. Jin,* M. Himuro,
Y. Yamamoto* ______ **5893 – 5896**

Triflic Acid Catalyzed Synthesis of Spirocycles via Acetylene Cations

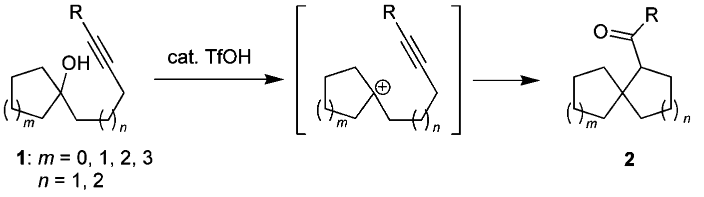

1: $m = 0, 1, 2, 3$
$n = 1, 2$

2

Rings of various shapes and sizes: Spirocyclic hydrocarbons **2** were obtained in good to excellent yield through the triflic acid (TfOH) catalyzed cyclization of alkynyl-substituted cyclic tertiary alcohols **1** under mild conditions with good control of ring size (see scheme). The method was extended to the synthesis of bridged bicyclic ketones with high stereoselectivity.

Direct Electron Transfer

O. Courjean, F. Gao,
N. Mano* ______ **5897 – 5899**

Deglycosylation of Glucose Oxidase for Direct and Efficient Glucose Electrooxidation on a Glassy Carbon Electrode

Down to the bare bones: When a glucose oxidase (GOx, left) was deglycosylated, the modified enzyme (right) immobilized on a vitreous carbon electrode came into closer electrical contact with the surface than the native enzyme. Glucose was electrooxidized directly on a monolayer of deglycosylated GOx on a carbon electrode at the unprecedented reducing potential of −200 mV versus Ag/AgCl and with a current density of 235 $\mu A\,cm^{-2}$.

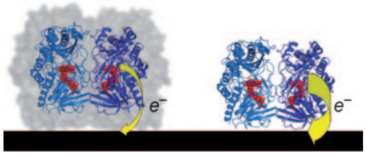

Insertion Reactions

R. A. Taylor, D. J. Law, G. J. Sunley,
A. J. P. White,
G. J. P. Britovsek* ______ **5900 – 5903**

Towards Photocatalytic Alkane Oxidation: The Insertion of Dioxygen into a Platinum(II)–Methyl Bond

Always look on the bright side: The light-driven insertion of dioxygen into a platinum–methyl bond results in a methylperoxo complex (see picture) which decomposes to formaldehyde and a platinum hydroxo complex. This reaction occurs at 1 atm O_2 and room temperature within minutes, and proceeds via the formation of singlet oxygen.

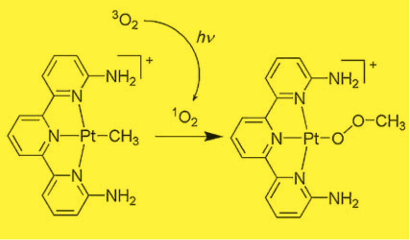

Halogenated Fullerenes

I. N. Ioffe, A. A. Goryunkov, N. B. Tamm,
L. N. Sidorov, E. Kemnitz,*
S. I. Troyanov* ______ **5904 – 5907**

Fusing Pentagons in a Fullerene Cage by Chlorination: IPR D_2-C_{76} Rearranges into non-IPR $C_{76}Cl_{24}$

Spectacular skeletal rearrangement of the C_{76} fullerene cage was observed as a result of chlorination of D_2-C_{76} to give $C_{76}Cl_{24}$ (see structure; gray C, green Cl, orange bonds highlight the pentagons), which features a significantly flattened carbon cage that violates the isolated pentagon rule. This transformation is likely to include seven single Stone–Wales rearrangements, which are facilitated by chlorination of the fullerene cage.

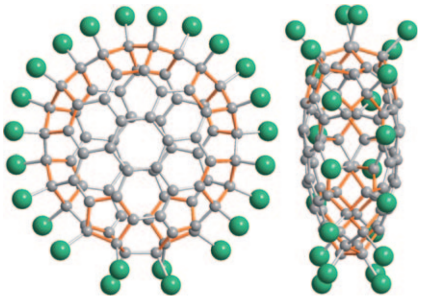

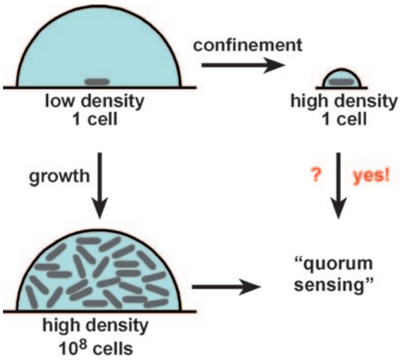

One is a quorum: As few as one to three cells of *Pseudomonas aeruginosa* bacteria are confined in small volumes by the use of microfluidics. These small numbers of cells are able to activate quorum sensing (QS) pathways and achieve QS-dependent growth. The results also show that at low numbers of cells, initiation of QS is highly variable within a clonal population.

Microfluidics

J. Q. Boedicker, M. E. Vincent,
R. F. Ismagilov* ———— **5908 – 5911**

Microfluidic Confinement of Single Cells of Bacteria in Small Volumes Initiates High-Density Behavior of Quorum Sensing and Growth and Reveals Its Variability

---

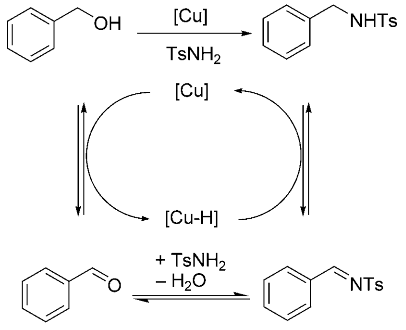

Water is the only by-product in an efficient and atom-economical $Cu(OAc)_2$-catalyzed coupling of alcohols with sulfonamides (see proposed mechanism; Ts = *p*-toluenesulfonyl). It was discovered that bissulfonylated amidines formed as intermediates when the transhydrogenative C–N bond-forming reaction is carried out in air act as novel ligands to stabilize the catalyst.

C–N Bond Formation

F. Shi,* M. K. Tse, X. Cui, D. Gördes,
D. Michalik, K. Thurow, Y. Deng,
M. Beller* ———— **5912 – 5915**

Copper-Catalyzed Alkylation of Sulfonamides with Alcohols

Clean and green: Copper(I) complexes of phenanthroline-based ligands anchored on the chitosan polymer are good catalysts for the "click" cycloaddition of azides with terminal alkynes (see scheme; the scanning electron microscopy image shows the porous structure of the catalyst). These heterogeneous catalytic systems do not require a base or reducing agent and operate in alcohol or water.

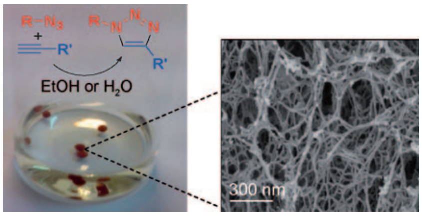

Heterogeneous Catalysis

M. Chtchigrovsky, A. Primo, P. Gonzalez,
K. Molvinger, M. Robitzer, F. Quignard,*
F. Taran* ———— **5916 – 5920**

Functionalized Chitosan as a Green, Recyclable, Biopolymer-Supported Catalyst for the [3+2] Huisgen Cycloaddition

---

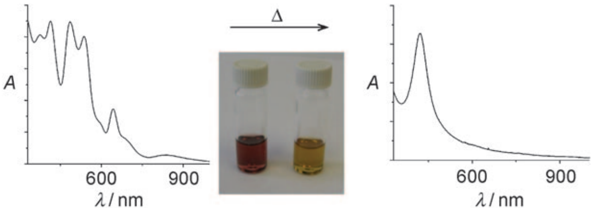

A simple one-pot method produces silver nanoparticles coated with aryl thiols that show intense, broad nonplasmonic optical properties. The synthesis works with many aryl-thiol capping ligands, including water-soluble 4-mercaptobenzoic acid. The nanoparticles produced show linear absorption that is broader, stronger, and more structured than most conventional organic and inorganic dyes.

Metal Nanoparticles

O. M. Bakr, V. Amendola, C. M. Aikens,
W. Wenseleers, R. Li, L. Dal Negro,
G. C. Schatz, F. Stellacci* —— **5921 – 5926**

Silver Nanoparticles with Broad Multiband Linear Optical Absorption

Homogeneous Catalysis

H. Van Nguyen, R. Matsubara,
S. Kobayashi* ________ **5927 – 5929**

Addition Reactions of Sulfonylimidates with Imines Catalyzed by Alkaline Earth Metals

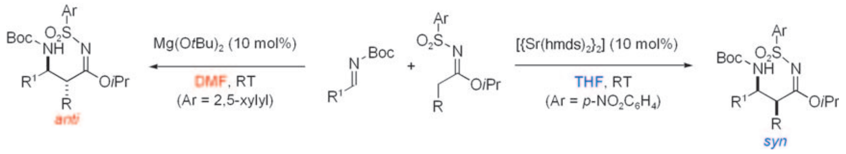

Cheaper, safer: Addition reactions of sulfonylimidates to imines are catalyzed by alkaline-earth-metal alkoxide salts, which are abundant, inexpensive, and nontoxic. Diastereoselectivity is highly dependent on solvent and catalyst, and both *syn* and *anti* adducts are obtained in high yields and with high diastereoselectivity (see scheme). The first catalytic asymmetric Mannich-type reaction of a sulfonylimidate is also presented.

Macromolecular Architectures

M. Schappacher,
A. Deffieux* ________ **5930 – 5933**

Imaging of Catenated, Figure-of-Eight, and Trefoil Knot Polymer Rings

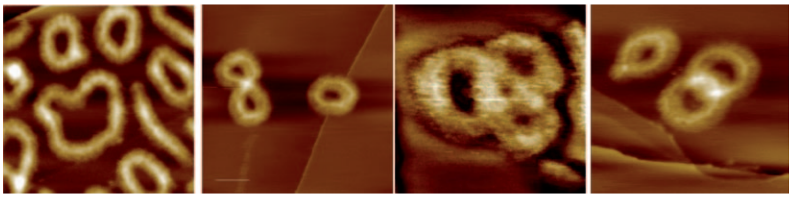

A knotty problem: Macrocyclic topological isomers formed during the end-to-end cyclization of linear polymer chains are imaged by using atomic force microscopy (AFM). Images of isolated molecules (see picture) were obtained after magnification of the initial polymer rings by grafting polystyrene oligomers to the macrocyles. This technique allows the visualization of nontrivial macrocyclic architectures.

Polyoxometalates

A. Müller,* F. L. Sousa, A. Merca,
H. Bögge, P. Miró, J. A. Fernández,
J. M. Poblet, C. Bo ________ **5934 – 5937**

Supramolecular Chemistry on a Cluster Surface: Fixation/Complexation of Potassium and Ammonium Ions with Crown-Ether-Like Rings

Integrated but separate: A strongly nucleophilic cluster surface allows the selective complexation and separation of ammonium and potassium ions. Six $\{Mo_4VKO_6\}$ rings with crown-ether-like functionality (see picture; Mo blue, V green, K pink, O red) present in the holes of the investigated cluster complex integrate six ammonium ions (N orange, H yellow).

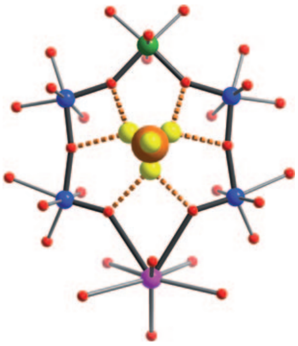

Solar Cells

H. Choi, S. O. Kang, J. Ko,* G. Gao,
H. S. Kang, M.-S. Kang,
M. K. Nazeeruddin,
M. Grätzel ________ **5938 – 5941**

An Efficient Dye-Sensitized Solar Cell with an Organic Sensitizer Encapsulated in a Cyclodextrin Cavity

Dying to get inside: Charge recombination is retarded and dye aggregation is prevented in solar cells that contain the JK-2 dye encapsulated in a cyclodextrin (CD) cavity (see picture). The β-CD/JK-2 device with a polymer gel electrolyte gave an overall conversion efficiency of 7.40%, which is the highest value reported to date for DSSCs based on the organic sensitizers, and showed excellent stability.

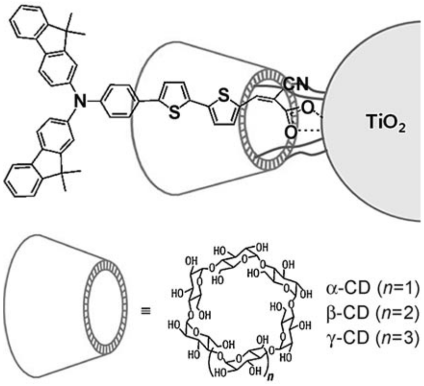

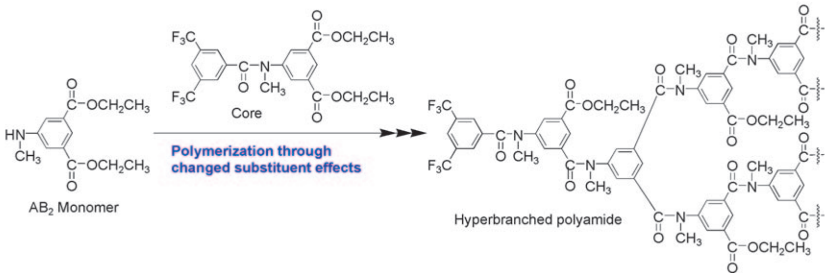

Branching out: Condensation polymerization of AB$_2$ monomer proceeds selectively from a core molecule owing to the change of substituent effects between the monomer and the polymer (see scheme). Hyperbranched polyamides are obtained with very low polydispersity and controlled molecular weight determined by the monomer/core feed ratio.

Hyperbranched Polymers

Y. Ohta, S. Fujii, A. Yokoyama,
T. Furuyama, M. Uchiyama,
T. Yokozawa* ______ **5942 – 5945**

Synthesis of Well-Defined Hyperbranched Polyamides by Condensation Polymerization of AB$_2$ Monomer through Changed Substituent Effects

---

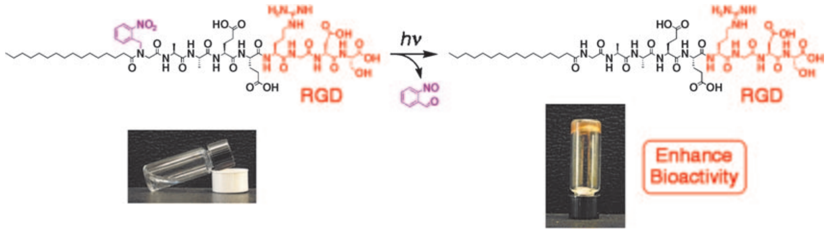

Photocleavage of a 2-nitrobenzyl group in a bioactive peptide amphiphile containing the Arg-Gly-Asp (RGD) epitope triggers a sol-to-gel transition as nanospheres are converted to nanofibers (see picture). This morphological change enhances the bioactivity of the nanostructures surrounding cells in three dimensions.

Nanostructures

T. Muraoka, C.-Y. Koh, H. Cui,
S. I. Stupp* ______ **5946 – 5949**

Light-Triggered Bioactivity in Three Dimensions

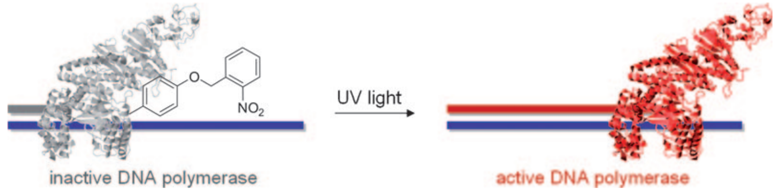

When the time is right: The widely applied *Thermus aquaticus* DNA polymerase was rendered light-activatable by incorporation of the photocaged amino acid *ortho*-nitrobenzyl tyrosine in place of a key tyrosine residue in the active site (see picture). As the modified enzyme was completely inactive until irradiated with UV light, temporal regulation of polymerase activity was possible.

Photocaging

C. Chou, D. D. Young,
A. Deiters* ______ **5950 – 5953**

A Light-Activated DNA Polymerase

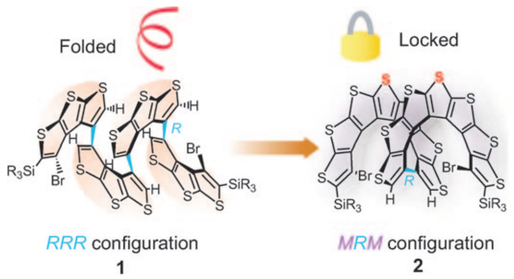

From helical folding to helical locking: Tetrakis(β-trithiophene) **1** folds into a helical conformation (*RRR*) that facilitates double ring annelation, with high diastereoselectivity and modest enantioselectivity, to provide bis[7]helicene **2** (*MRM*). This rigid, helically locked structure has enhanced chiroptical properties similar to the corresponding [15]helicene.

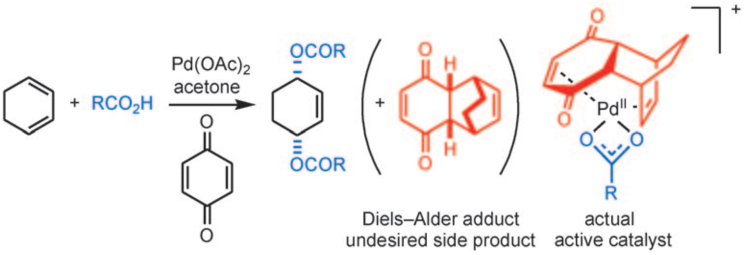

Side products get involved: The 1,4-oxidation of a diene transforms a simple hydrocarbon into an extremely useful intermediate. A complex formed in situ between palladium and a bicyclic Diels–Alder adduct, which is produced as a side product during the reaction, was responsible for the high rate and high diastereoselectivity observed in the oxidation of cyclohexadiene (see scheme).

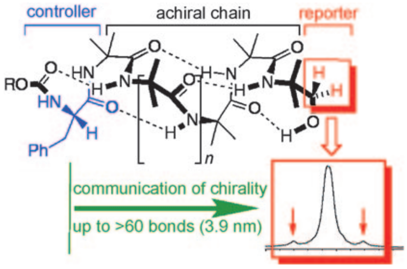

Successful communication: Two diastereotopic protons more than 60 bonds from the nearest chiral center appear as an AB system, showing that the intervening structure is a well-ordered helix. Decay of anisochronicity quantifies the linear persistence of a helix of achiral amino acids: as little as 3.5 % of the chiral influence is lost with each additional achiral residue.

Supporting information is available on www.angewandte.org (see article for access details).

A video clip is available as Supporting Information on www.angewandte.org (see article for access details).

Service

Corrigendum

The authors of this Communication have recognized an error in Equation (2). The correct Equation (2) is therefore as follows:

$$\chi_M = \frac{1}{k_B\,(T-\theta)}\,\frac{2\,N_A\,g^2\,\mu_B{}^2}{3+\exp\left(-\frac{2J}{k_B\,T}\right)} \qquad (2)$$

Moreover, in the right-hand column on page 923, the optimized value for the exchange coupling J should be corrected to $J = 11.2\ \mathrm{cm^{-1}}$ ($= 16.0$ K), and Ref. [3] cited in this paragraph should be Ref. [6].

A Spiro-Fused Triarylaminium Radical Cation with a Triplet Ground State

A. Ito, M. Urabe, K. Tanaka* — **921–924**

Angew. Chem. Int. Ed. **2003**, *42*

DOI 10.1002/anie.200390244